Iterative Conversion of Cyclin Binding Groove Peptides into Druglike CDK Inhibitors with Antitumor Activity

Padmavathy Nandha Premnath,[†] Sandra N. Craig,[†] Shu Liu,[†,§] Erin L. Anderson,[†] Asterios I. Grigoroudis,[‡] George Kontopidis,[‡] Tracy L. Perkins,[†] Michael D. Wyatt,[†] Douglas L. Pittman,[†] and Campbell McInnes*,[†]

[†]Department of Drug Discovery and Biomedical Sciences, South Carolina College of Pharmacy, University of South Carolina, Columbia, South Carolina 29208, United States

[‡]Department of Biochemistry, Faculty of Veterinary Science, University of Thessaly, Trikalon 224, Karditsa 43100, Greece

Ⓢ *Supporting Information*

ABSTRACT: The cyclin groove is an important recognition site for substrates of the cell cycle cyclin dependent kinases and provides an opportunity for highly selective inhibition of kinase activity through a non-ATP competitive mechanism. The key peptide residues of the cyclin binding motif have been studied in order to precisely define the structure−activity relationship for CDK kinase inhibition. Through this information, new insights into the interactions of peptide CDK inhibitors with key subsites of the cyclin binding groove provide for the replacement of binding determinants with more druglike functionality through REPLACE, a strategy for the iterative conversion of peptidic blockers of protein−protein interactions into pharmaceutically relevant compounds. As a result, REPLACE is further exemplified in combining optimized peptidic sequences with effective N-terminal capping groups to generate more stable compounds possessing antitumor activity consistent with on-target inhibition of cell cycle CDKs. The compounds described here represent prototypes for a next generation of kinase therapeutics with high efficacy and kinome selectivity, thus avoiding problems observed with first generation CDK inhibitors.
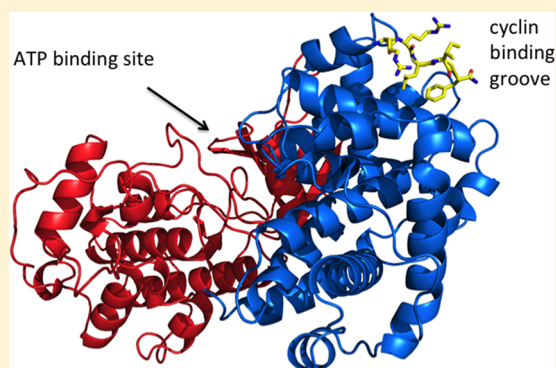
INTRODUCTION

Cyclin dependent kinases (CDKs) and their natural inhibitors (CDKIs) are central to cell cycle regulation, and their functions are commonly altered in tumor cells.[1] Deregulation of CDK2 and CDK4 through inactivation of CDKIs such as p16[INK4a], p21[WAF1] (p21), p27[KIP1], and p57[KIP2] provides a means for cancer cells to override the G1 checkpoint.[2,3] Compounds that mimic the ternary complex of CDKIs with CDK/cyclins should lead to reinstatement of CDK inhibition and therefore represent an opportunity for pharmacological interference with tumor progression.[4,5] A particular hypothesis for tumor selective cell death through inhibiting the phosphorylation of CDK substrates comes from observations that the CDK2/cyclin A (CDK2A) complex is a key regulator of E2F1 transcriptional activity.[6] E2F activity must be terminated in a timely fashion during S-phase, as persistent function results in a powerful apoptotic signal mediated by transcriptional effects.[7] Inhibition of CDK activity with cyclin groove inhibitors (CGI) therefore results in tumor selective induction of apoptosis in cells already possessing deregulated E2F.[8−10]

CDK2 activity appears to be redundant for the proliferation of normal cells and in some cases for cancer cells, leading to doubts as to the validity of CDK2 as a drug target. Studies suggest that its nonessential role is a result of the substitution of one CDK for another.[1,11−13] This can occur, since the various CDK isoforms are in high abundance throughout the cell cycle and are transiently activated by cyclin binding and subsequent phosphorylation. Inhibition of the cell cycle CDKs through the cyclin groove rather than the ATP binding site offers the possibility to overcome the switch to a different CDK family member when the activity of one particular isoform is downregulated. As the transient expression of a specific cyclin is obligatory both for activation of the kinase and for substrate recruitment of critical cell cycle regulatory proteins and resulting progression, the cancer cell will be unable to bypass CDK activity directly. It is believed that a component of the anticancer activity of CDK inhibitors is through the transcriptional inhibition of CDK7 and CDK9.[14,15] While it has been suggested that transcriptional CDK inhibition may be beneficial for cancer therapy, it is also probable that this will lead to significant toxicities and has led to the failure of CDK2 inhibitors in clinical trials. Targeting of the protein−protein

Table 1. Structure−Activity Relationship of p21 and p107 Derived Peptide Analogs

betahomoleucine (βleu)   3-thienylalanine (3TA)   cyclohexylalanine (CHA)
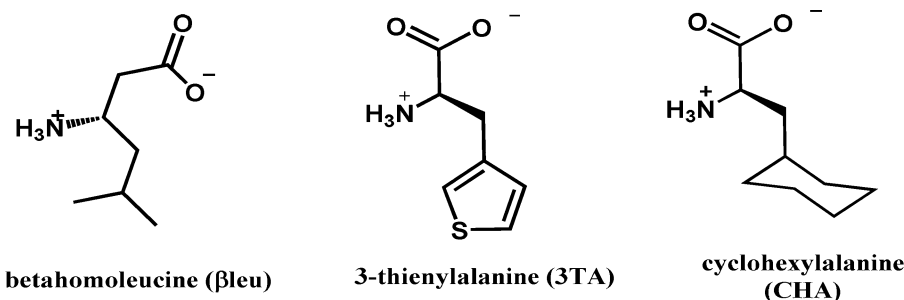
ID	Peptide sequence	CDK2A IC$_{50}$(μM)	CDK4D IC$_{50}$ (μM)
1	SAKRRLFG-NH2	0.07±0.02	0.88±0.34
2	SAKRRLFG	0.05±0.02	0.66±0.21
3	SAKRRL{3TA}G	0.18±0.07	1.67±0.53
4	SAKRR{βLeu}FG	0.02±0.003	0.29±0.07
5	SAKRR{βLeu}{3TA}G	0.01±0.002	0.04±0.007
6	SAKRNLFG-NH2	0.24±0.11	3.09±2.00
7	HAKRRLI{CHA}	0.02±0.004	0.18±0.04
8	HAKRRLIF	0.02±0.01	0.12±0.05

interaction involved in CDK2 substrate recruitment therefore offers the possibility of generating cell cycle selective CDK inhibitors. With only cyclins A, D, and E containing a functional cyclin binding groove (CBG), it is possible in principle to inhibit the G1 and S phase CDKs (CDK2, -4, and -6) selectively while avoiding those involved in transcriptional regulation. Cyclin groove inhibitors should therefore avoid undesirable side effects of ATP competitive CDK inhibitors.[16,17] Highly potent peptidic inhibitors of CDK activity have been described and in cell permeable form result in antitumor activity therefore providing proof of concept for non-ATP competitive targeting.[8,10]

To exploit protein−protein interactions as drug targets, REPLACE, a unique drug discovery strategy has been validated and applied to discover first generation inhibitors of the cyclin groove that serve as the basis for oncology drug development.[18−21] Further progress in delineating the structure−activity of such inhibitors is described here providing essential information for the conversion of peptides into nonpeptidic molecules. Modification of CGI compounds was successfully undertaken through the principles of REPLACE resulting in optimized inhibitors with enhanced druglike properties, anticancer activity, and confirmation of on-target mechanism of action through cell cycle analysis.
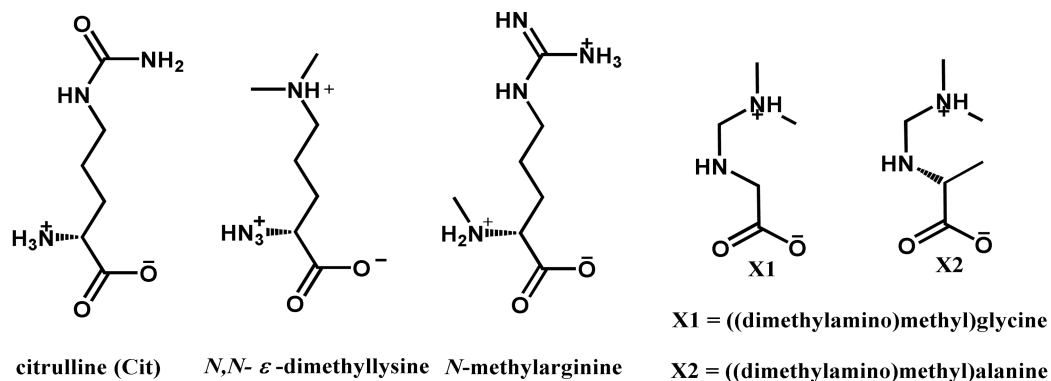
■ RESULTS

Structure−Activity Relationship of Octapeptide Analogs. While structure−activity relationships for the cyclin binding motif (CBM) have previously been described, contributions of key residues have not been adequately investigated.[22−24] In addition, analysis is required to determine the consequences of these substitutions in the context of smaller peptides that are a starting point for drug discovery. Furthermore, detailed structure−activity relationships have

been conducted in both CDK2/cyclin A (CDK2A) and CDK4/cyclin D1 (CDK4D) contexts which has not been previously carried out. To this end, peptides derived from p21 (CDK inhibitory protein) and p107 (Rb like substrate) were modified to study the key determinants of binding. These include an acidic region of the cyclin binding groove interacting with basic residues of the CBM, and two hydrophobic pockets, the larger of which interacts with the C-terminal LIF and LFG motifs. Since detailed SAR information is a key component of REPLACE, two peptide sequences were chosen as the basis for these modifications and included SAKRRLFG (p107 derived) and HAKRRLIF (optimized p21 octapeptide). For these octapeptides, substitutions and deletions of the C-terminal motif were undertaken to study the binding requirements for CDK2A and CDK4D and to probe structural differences of the major hydrophobic pocket in each cyclin context. Peptide activity (Table 1) was quantified with a competitive binding assay previously described employing fluorescence polarization (FP) of a fluorescein labeled octapeptide as the readout.[18]

In the first instance, the contributions of the C-terminal residues and functional groups were explored. SAKRRLFG-NH$_2$ (**1**) and SAKRRLFG-OH (**2**) were synthesized and shown to have comparable binding activity for CDK2A (0.07 vs 0.05 μM) and CDK4D (0.88 vs 0.66 μM), suggesting that the amide and carboxylic acid groups interact similarly in both contexts. 3-Thienylalanine (3TA, **3**) was incorporated as a substitution for Phe8 and found to be a successful non-natural replacement. In the FP assay, the activity of this compound was determined to be 0.18 μM for CDK2A and 1.67 μM for CDK4D, suggesting a 2-fold decrease in binding to both contexts.

β-Homoleucine (β-Leu) was hypothesized as an efficient way of mimicking the spacing functionality of the Ile residue in the LIF motif of the p21 sequence and improving binding activity

Table 2. Cyclin A/CDK2 and Cyclin D1/CDK4 Binding Activity for Arg Replacement Peptides

citrulline (Cit) *N,N*-ε-dimethyllysine *N*-methylarginine

X1 = ((dimethylamino)methyl)glycine

X2 = ((dimethylamino)methyl)alanine

ID	Sequence	CDK2A IC$_{50}$ (µM)	CDK4D IC$_{50}$ (µM)
8	$H_1A_2K_3R_4R_5L_6I_7F_8$	0.02±0.01	0.12±0.05
9	RRLIF	1.01±0.17	25.12±2.97
10	Cit-RLIF	43.17±8.77	40.46±1.07
11	RCitLIF	5.19±1.56	15.76±1.94
12	R(dimethylLys)LIF	20.62±2.57	33.76±10.72
13	R(NMeArg)LIF	1.70±0.76	9.19±2.18
14	RPLIF	>180	>100
15	RGLIF	>180	>100
16	RALIF	20.36±7.57	28.76±12.86
17	R-X1-LIF	>180	>100
18	R-X2-LIF	>180	>100

of LFG containing peptides. Preliminary proof of concept for this has been previously obtained.[25] Exploring the β-Leu replacement in the p107 context (SAKRR[βLeu]FG, **4**) showed a 2- to 3-fold potency increase relative to the native Leu residue (**2**) in both cyclin contexts. Further to this, the β-Leu substitution was examined in the 3TA containing peptide. A dramatic enhancement in binding affinity for CDK2A was also determined for SAKRR{βLeu}{3TA}G (**5**) with an 18-fold increase in potency observed compared to **3**. Replacement of Arg5 with Asn (**6**) resulted in a 3- to 4-fold decrease in binding in both contexts. Cyclohexylalanine was found to be another effective replacement for phenylalanine (**7**) as part of the p21 derived peptide HAKRRLIF. Compound **7** had an IC$_{50}$ value of 0.02 µM for CDK2A and 0.18 µM for CDK4D, indicating very potent binding affinity to both CDK protein complexes and comparable contribution to the native residue in HAKRRLIF (**8**).

In order to further validate key leads and control compounds, their activity was examined in a direct binding format. Recently a protocol has been developed for soluble expression of monomeric cyclin A2 (174−432 fragment) and its activity confirmed using control compounds in an intrinsic tryptophan assay (manuscript in preparation). In this case binding to the cyclin groove is directly quantified by measuring fluorescence of Trp217, the only such residue in cyclin A. By use of this method, compound **8** was found to have a K_d value of 0.019 ± 0.004 µM and therefore was very similar to the result obtained in the FP competitive binding assay validating both sets of observed activities.

Structure−Activity Relationship of Pentapeptide Analogs Based on p21. Further to the studies exploring SAR in the p21 and p107 octapeptide sequences, more detailed investigation into the positional requirements of smaller peptides was completed (Table 2). The truncated p21 pentapeptide RRLIF was selected as representing a realistic size and molecular weight for conversion to more druglike compounds through the REPLACE strategy (Figure 1). Three series of peptide analogs derived from RRLIF (**9**, IC$_{50}$ = 1.01 µM and IC$_{50}$ = 25.12 µM for CDK2A and CDK4D, respectively) were designed to introduce replacements for key binding determinants. Both natural and non-natural amino acid alternatives for Arg4, Arg5, Leu6, and Phe8 were incorporated to examine the sensitivity and requirement for binding to the CBG.

To examine the sensitivity of the critical Arg4 position, substitution of this residue with citrulline in Cit-RLIF (**10**) was undertaken to probe the replacement of the salt bridge interaction of the highly basic guanidinium side chain with the noncharged urea isostere. The resulting activity data showed a substantial potency decrease of 40-fold with CDK2A (43.17 µM) but a lesser impact for the CDK4D context (3 fold decrease, 40.46 µM).

Further to this, a number of exploratory substitutions were incorporated at the Arg5 position which has previously been shown to be less sensitive to substitution than Arg4.[24,25] The citrulline replacement at this position (**11**) confirmed this with activity values of 5.19 µM for CDK2A and 15.76 µM for CDK4D, suggesting a 5-fold decrease in affinity compared to RRLIF and an increase in binding to CDK4D. Substitution with
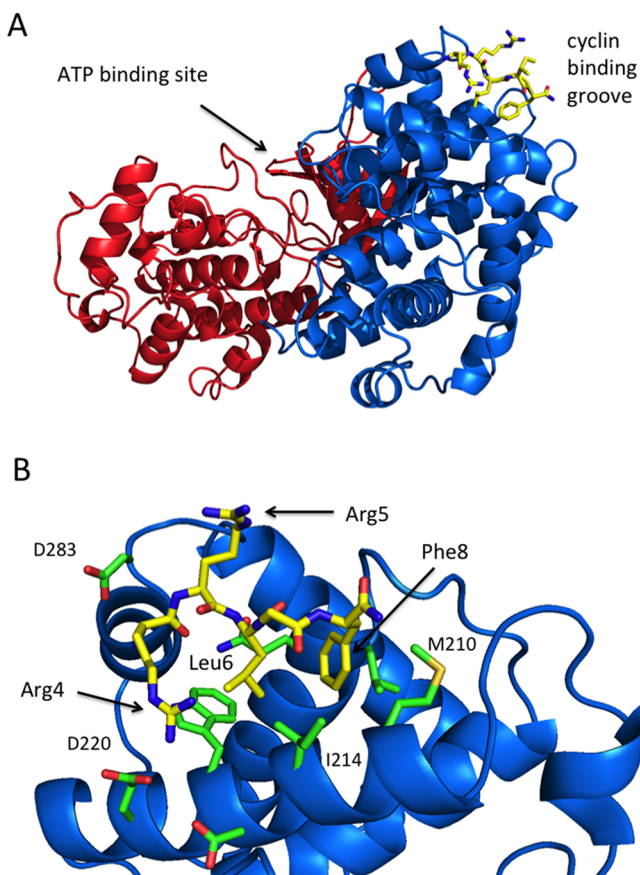
A

B

Figure 1. Complex of RRLIF and CDK2/cyclin A. (A) Tertiary structure of CDK2 (red ribbon), cyclin A (blue ribbon), and RRLIF (**9**) bound to the cyclin groove. (B) Close-up view of the interactions of RRLIF with the cyclin groove where **9** (yellow carbons) and the key interacting side chains of cyclin A (green carbons) are shown as a stick representation. Residues of the peptide are indicated by three-letter amino acid code, whereas those of the protein are labeled with one-letter codes.

isosteric non-natural amino acids including lysine with dimethylation of the ε-amino group (**12**; R(N,N-ε-dimethyllys)LIF, IC$_{50}$ = 20.62 μM) resulted in approximately 20-fold potency loss against CDK2A. Incorporation of N-Me Arg (**13**, R(NMeArg)LIF, 1.70 μM) suggests that backbone methylation of this residue does not affect activity and with CDK4D improves potency by 2-fold (Table 2).

In further studies of the tolerance of Arg5 substitution for binding to the cyclin groove, nonconservative mutations were incorporated (Table 2). Proline substitution (**14**, RPLIF) was shown to be detrimental to activity with IC$_{50}$ values greater than 100 μM for both CDK/cyclin complexes. Glycine substitution (**15**) led to a similar activity cliff. The alanine surrogate (**16**, RALIF) retained some activity with a competitive binding IC$_{50}$ of just over 20 μM in both contexts, a respectable value considering the loss of ion-pairing capability. In order to examine the structural basis for the potency variations upon modification of the peptide sequences, a computational approach was used to model the interactions of each peptide in this study. The complex of RRLIF bound to CDK2A has been previously determined (1OKV) and was therefore used for binding mode analysis and interaction energy calculations. The competitive binding efficiency for each peptide substitution as determined by FP assay was compared

with the interaction energy obtained for the peptide complexes with CDK2A, and a good correlation between these two parameters was observed with an R^2 value of 0.855 as shown (Figure 2). These results demonstrate that the loss of ion
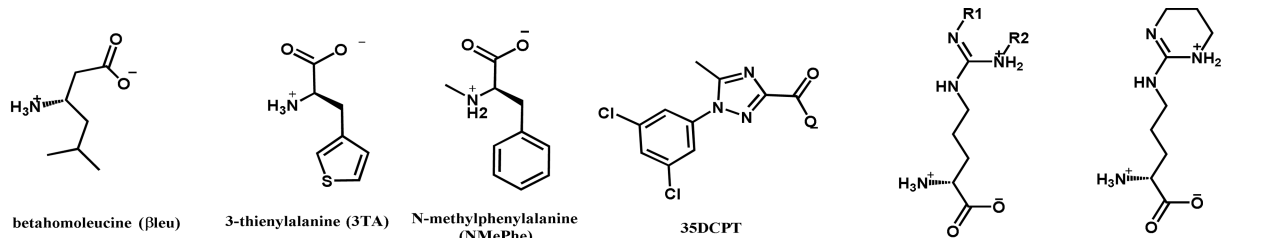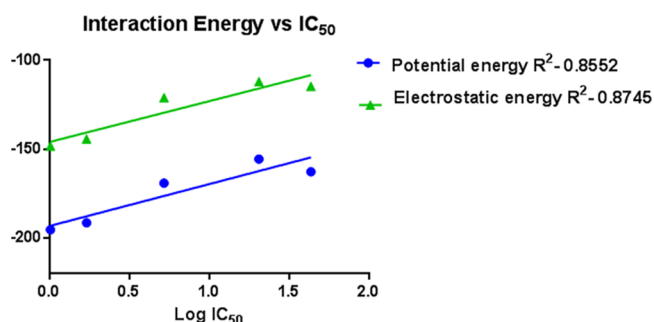

Figure 2. Correlation of the interaction energies calculated for the peptide analogs tested in Table 2 with the experimental affinity values as measured by inhibition constants determined using the FP binding assay. The correlation observed (R^2 = 0.857) suggests that the computational method is predictive of actual binding.

pairing interactions occurring in the citrulline and other nonconservative replacement derivatives was accurately reflected in the obtained interaction energy values. These also suggest that prospective modeling of additional mutations and capping group substitutions will be possible by computational design.

Further to the exchanges of natural and non-natural amino acids for the second arginine (Arg5), peptoid substitutions were utilized in order to stabilize the backbone of the CGI compound and to probe the consequence of shifting the side chain one atom toward the N-terminus. Two different peptoids incorporating a dimethylamino methyl group (Table 2, **17**, X1 = (2-(dimethylamino)methyl)glycine) and (**18**, X2 = (2-(dimethylamino)methyl)alanine) were synthesized. Neither of these peptide−peptoid hybrids displayed measurable binding activity for CDK2A or CDK4D, suggesting nonoptimal positioning of the basic group for ion-pairing with the cyclin.

Subsequent to the SAR investigation of the N-terminal arginines, residues of the C-terminal region were replaced by non-natural amino acids and furthermore were deleted and/or truncated in the p21 and p107 contexts (Table 3). Previous comparisons of the p21 and p27 C-termini indicate that placement of a spacer residue between the leucine and phenylalanine results in a considerable potency increase due to more optimal complementarity of the lipophilic side chains with the primary hydrophobic pocket. RRLFG (**19**, IC$_{50}$ = 18.88 μM) was synthesized and tested to further examine impact on binding to cyclin A and D and was found to undergo greater than 10-fold decrease in potency. Truncation of the C-terminal glycine resulted in even weaker CDK2A binding (**20**, IC$_{50}$ = 35.65 μM). These results suggest a significant impact of deletion of the spacer residues in both scenarios. To further underscore the importance of spacing for optimal positioning of the two side chains, incorporation of β-Leu as a leucine replacement resulted in recapitulation of activity for both CDK2A (RRβLeuF, **21**, IC$_{50}$ = 2.81 μM) and CDK4D (21.17 μM). Readdition of the glycine residue resulted in a slight further potency improvement (RRβLeuFG, **22**;, IC$_{50}$ = 1.73 μM CDK2/cyclin A, 20.24 μM CDK4D). Interchange of the native residue with 4-fluorophenylalanine generated a 2-fold binding increase to both CDK/cyclin complexes (RRLNpfF,

Table 3. Conversion of p21 Peptides into More Druglike Cyclin Groove Inhibitors

betahomoleucine (βleu) 3-thienylalanine (3TA) N-methylphenylalanine (NMePhe) 35DCPT

G10 R$_1$=CH$_3$, R$_2$=H
G11 R$_1$=CH$_3$, R$_2$=CH$_3$
G12 R$_1$=CH$_2$CH$_3$, R$_2$=H

G19

ID	Sequence	CDK2A IC$_{50}$ (µM)	CDK4D IC$_{50}$ (µM)	ClogP	tPSA	MTT IC$_{50}$ (µM), U2OS	MTT IC$_{50}$ (µM), DU145
9	RRLIF	1.01±0.17	25.12±2.97	-2.75	303		
19	RRLFG	18.88±4.45	>100				
20	RRLF	35.65±10.51	>100				
21	RR{βLeu}F	2.81±0.76	21.17±2.99				
22	RR{βLeu}FG	1.73±0.46	20.24±5.37				
23	RRLNpfF	0.70±0.19	9.26±2.07				
24	RR{βLeu}{NMeF}	1.35±1.38	45.58±5.63				
25	RR{βLeu}{NMeF}-NH$_2$	5.82±3.12	81.13±3.78	-2.04	271		
26	35DCPT-Cit{βLeu}{NMeF}-NH$_2$	>100	>100			>100	>100
27	35DCPT-R{βLeu}{NMeF}-NH$_2$	8.95±4.15	78.25±11.09	3.25	211	30.7±2.7	36.5±2.6
28	35DCPT-R{βLeu}{3TA}-NH$_2$	5.70±3.55	>100	2.57	220	18.3±1.5	21.8±0.32
29	35DCPT-G10-{βLeu}{3TA}-NH$_2$	46.75±10.68	>100			>100	>100
30	35DCPT-G11-{βLeu}{3TA}-NH$_2$	3.69±0.23	>100			75.6±1.2	102±14
31	35DCPT-G12-{βLeu}{3TA}-NH$_2$	16.39±3.72	>100			108±4	130±27
32	35DCPT-G19-{βLeu}{3TA}-NH$_2$	4.50±0.74	>100			60.5±3.3	81±8

23, IC$_{50}$ = 0.70 µM CDK2/cyclin A, 9.26 µM CDK4D). In order to improve the druglikeness and metabolic stability of the peptidic compounds, *N*-methylphenylalanine was used as a replacement in the context of the βLeu while also exploring the role of the C-terminal functional group. RR{βLeu}NMeF-OH (**24**, IC$_{50}$ = 1.35 µM) and R{βLeu}NMeF-NH$_2$ (**25**, IC$_{50}$ = 5.82 µM) showed that N-methylation of the Phe backbone resulted in greater inhibition of CDK2A.

Synthesis and Antitumor Effects of Druglike Cyclin Groove Inhibitors. In previous work, it was shown that capping groups based upon a 1-(phenyl)-5-methyl-1*H*-1,2,4-triazole-3-carboxylic acid core structure represent effective replacements for the N-terminal tetrapapetide of HAKRRLIF and in the context of the capped tetramer (RLIF) result in similar activity to the p21 pentapeptide.[18] With this knowledge in hand, N-capped tripeptides were synthesized incorporating SAR information described in the previous section, and their binding to CDK2A was measured (Figure 3, Table 3). These included the 1-(3,5-dichlorophenyl)-5-methyl-1*H*-1,2,4-triazole-3-carboxamide (35DCPT) N-capped peptides, 35DCPT-Cit-βLeu-NMePhe (**26**, IC$_{50}$ >100 µM), 35DCPT-Arg-βLeu-NMePhe (**27**, IC$_{50}$ = 8.95 µM), and 35DCPT-Arg-βLeu-3TA (**28**, IC$_{50}$ = 5.70 µM). Results indicate that comparable levels of potency to the parent peptide **9** were obtained with N-capped molecules (see **25**). Incorporation of citrulline in this context however results in a substantial decrease in binding for CDK2A relative to the peptides (see **11**). Binding of these CGI compounds to CDK4D was much lower with little activity being observed at relatively high concentrations of inhibitor. Because of their overall improved druglikeness through inclusion of nonpeptidic, non-natural amino acid components,
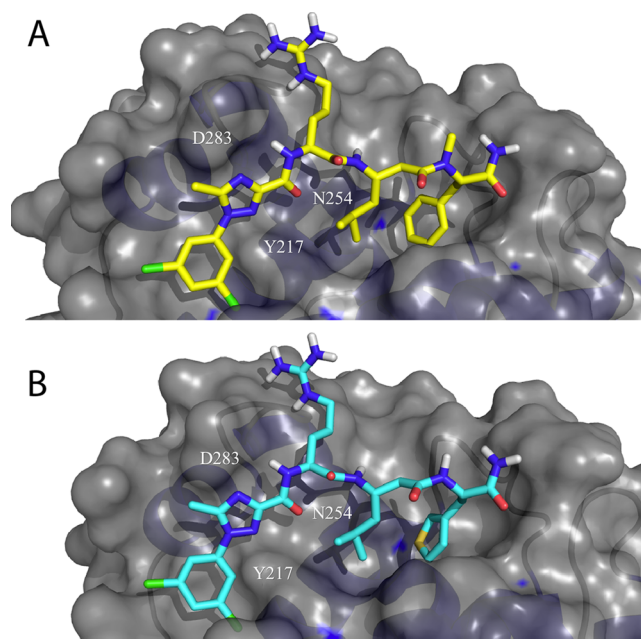

Figure 3. Binding mode of two druglike cyclin groove inhibitors. (A) **27** (yellow carbon atoms) showing the N-methylated phenylalanine residues and (B) **28** (cyan carbon atoms) illustrating the 3-thienylalanine residue. Both compounds are displayed interacting with the solvent accessible surface of cyclin A and where the west part of the molecule binds to the minor pocket and the second arginine binding site whereas the east side interacts with the major lipophilic site.
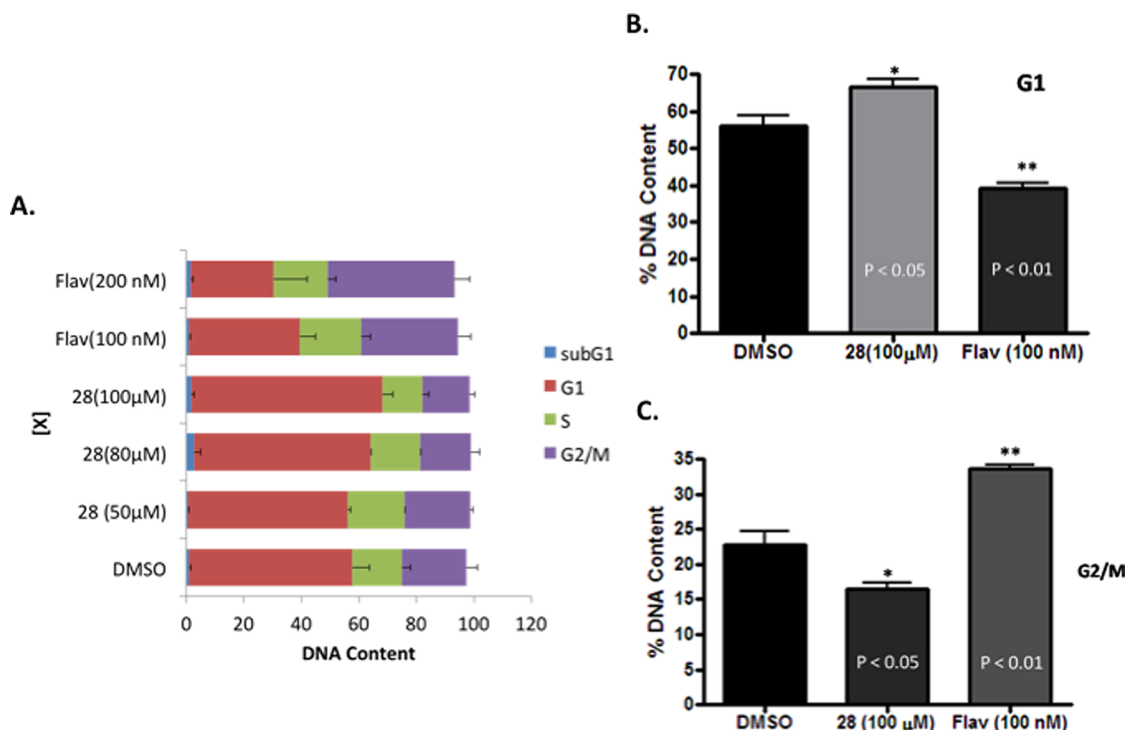
Figure 4. Cell cycle analysis of asynchronous U2OS cells treated with flavopiridol and **28**. U2OS cells were treated for 48 h, with DMSO only as a control, and adherent cells were fixed with 70% ethanol and stained with DAPI (4′,6-diamidino-2-phenylindole). Samples were analyzed by FACS and were performed in triplicate with a one-way ANOVA statistical analysis. (A) Analysis of total DNA content. (B) Comparison of percentage of cells in G1. (C) Comparison of percentage of cells in G2.

the three N-capped tripeptides were tested for preliminary antitumor effects in a cellular viability assay. Growth inhibition values obtained in the MTT assay demonstrated that significant antiproliferative activity was observed in two tumor cell lines. IC_{50} values in U2OS osteosarcoma and DU145 prostate tumor cells (Table 3) were found for **27** (30.7 and 36.5 μM, respectively) and **28** (18.3 and 21.8 μM, respectively) with the 3TA containing molecule being the most potent. Not surprisingly the decreased on-target activity and different physicochemical properties of the citrulline containing compound (**26**) led to no observable cellular activity.

As an extension of the preliminary data indicating the successful conversion of the p21 peptide RRLIF into a more druglike inhibitor, further modification and optimization of structure were undertaken (Table 3). It has been reported that incorporation of modified arginine derivatives into peptides results in enhancements both in ion-pairing ability and in cell permeability.[26] A series of non-natural isosteric analogs were included based on the concept that steric inhibition of aqueous ion solvation through guanidine alkylation promotes ion-pairing interactions. In addition, increased lipophilicity of the non-natural residues may improve pharmacokinetic parameters. As shown (Table 3), the modified Arg5 residues were included as derivatives of **28** containing the 3-thienylalanine, where the guanidine group is monomethylated (G10, **29**, IC_{50} = 46.75 μM), dimethylated (G11, **30**, IC_{50} = 3.69 μM), monoethylated (G12, **31**, IC_{50} = 16.39 μM), and cyclized (G19, **32**, IC_{50} = 4.50 μM). Evaluation of these compounds in the FP assay revealed that the dimethyl and cyclic guanidines had an approximately 2-fold enhancement in potency confirming that the greater magnitude of the charge−charge interaction improved binding. Testing of these compounds in the MTT assay however did not result in a corresponding increase in activity (Table 3) relative

to **28** and conversely seemed to diminish the antiproliferative effect, thereby suggesting that in this context, the alkylated guanidines did not lead to improvements in cellular permeability.

Previous attempts at studying cellular effects and consequences of cyclin groove inhibition centered on the use of chimeric peptides derived from p27 with penetration enhancing sequences appended to the N-terminus. Minimal mechanistic data resulted from the use of these peptides; however, significant antiproliferative activity was observed.[8,9] As described above, the cell permeable compounds developed in this study are the first true mechanistic probes of the consequences of CDK inhibition through the CBG and are therefore highly useful tools in validating cell cycle CDKs as antitumor therapeutics. In order to determine these effects in detail, cell cycle analysis through fluorescence activated cell sorting was carried out using the cell active N-capped tripeptides (Figure 4). The data obtained for **28** demonstrated an effect upon cell cycle distribution that is consistent with inhibition of CDKs that play a key role in regulating the checkpoints. Relative to the DMSO control, a dose dependent G1 arrest was observed in asynchronous U2OS cells after treatment with **28** in contrast to the effect observed for flavopiridol which resulted in a G2/M accumulation. The latter result is consistent with previously published data for pan CDK inhibitors.[1]

■ DISCUSSION

The overarching objective of this study is to convert peptidic molecules based on the cyclin binding motif into more druglike compounds. As described above, REPLACE is an iterative approach that requires in the first instance a detailed structure−activity relationship for binding of a peptide to its target. In

addition, an in depth understanding of the structural basis for peptide affinity to its receptor is important. This information is crucial to decide which determinants can be truncated and to inform the discovery of fragment alternatives (capping groups) to replace the essential residues. Therefore, in order to lay the groundwork for further conversion of p21 and p107 peptides into compounds with more appropriate pharmaceutical properties, the structure−activity was determined for key binding determinants of these sequences. Natural and non-natural residues were incorporated, and both conservative (isosteric) and nonconservative mutations were explored to precisely define the roles of the parent amino acid in binding. This was done to expand the SAR information and especially for the pentapeptide series that requires transformation into more druglike compounds. Furthermore, limited data are available regarding the inhibition of CDK4/6 through the cyclin groove. This study addresses these issues and allows development of druglike inhibitors based on cyclin groove inhibition.

The CBG is primarily a hydrophobic groove consisting of a major and a minor site interacting with lipophilic side chains through the hydrophobic effect and van der Waals interactions (Figure 1). In addition, an acidic component of the binding interface (Glu220, Glu224, and Asp283; cyclin A2 numbering) surrounds the minor hydrophobic pocket and interacts with basic residues (His, Lys, and Arg) on CDK substrates through ion pairing contacts. Hydrogen bonding interactions of the peptide backbone amide groups are formed with various side chains of the cyclin (including W217 and Q254) and make significant contributions to affinity of the peptide inhibitor.

In the CDK2A context, replacement of the guanidinium group with the noncharged isosteric residue citrulline (Table 2) resulted in a 40-fold potency decrease for Arg4 and only a 4-fold decrease for Arg5. This is consistent with previous data suggesting a large contribution of Arg4 to binding by way of its multiple ion pairing interactions with the cyclin.[22] In contrast, only a 2-fold decrease in potency was observed for replacement of Arg4 and even a slight increase in binding for Arg5 in terms of CDK4D inhibition (Table 2). This indicates a diminished role of the critical arginine in the binding to cyclin D1 and is consistent with the absence of one of the critical ion pairing residues compared to cyclin A. Examination of crystal structures shows that cyclin D has a threonine residue in place of an aspartate (T62 vs D216). These results were further supported through computational studies and reflected in the calculated interaction energy values (Figure 2) for peptide analogs. Incorporation of N,N-Σ-dimethyllysine into the p21 pentapeptide resulted in greater loss of activity toward CDK2A than does the replacement with citrulline. This suggests that despite the presence of an ion pairing group, its position and the steric hindrance of the two methyl groups are unfavorable for binding. Replacement again is tolerated to a greater degree than in the cyclin D context, suggesting a larger volume of the binding pocket compared to cyclin A. Because of the important contributions of the side chain of Arg5 to binding, to determine the contribution of its amide NH group, and to stabilize the peptide toward proteolysis, synthesis of an N-methylated arginine containing p21 peptide was undertaken. As this modification was shown to have little impact toward binding in both cyclin contexts and even improved interaction with CDK4D by 2-fold, highly useful information was obtained for improving druglikeness of cyclin groove inhibitors requiring the guanidinium side chain.

Nonconservative proteinogenic amino acid alternatives for the Arg5 including Gly, Ala, and Pro for the most part were ineffective replacements due to loss of ion-pairing and H-bond interactions. The complete loss of binding through proline incorporation almost certainly results from the inability of this constrained residue to adopt the required binding conformation with the loss of backbone H-bonding potentially contributing also. Again, the experimental binding observations were validated structurally in modeling of these arginine replacements and in terms of the predicted binding of the substituted peptides (Figure 2, Supporting Information).

As a next step, Arg5 was replaced with a peptoid residue to incorporate a dimethylaminomethyl (DMAM) group through N-alkylation (Table 2). Inclusion of a peptoid moiety is a promising strategy to retain peptide-like functionality while at the same time improving overall stability. Since the side chain is moved from the α carbon onto the nitrogen, a tertiary amide resistant to proteolysis will be formed upon coupling. DMAM was incorporated into the pentapeptide as a substitution for Arg5 in both a glycine and alanine context. The loss of activity for both molecules (17 and 18) most likely stems from the steric and conformational properties of the resulting molecule, despite the modeling results and design suggesting the close interaction of the basic nitrogen of the DMAM group with Asp283 (Figure 1). Further refinement of the side chain spacer may result in improvements in binding however.

As discussed above, Leu6 and Phe8 of the C-terminal motif are critical for binding as shown by replacement with alanine and through observed contacts of these residues with the primary hydrophobic pocket (Table 3). In the p21 sequence, Ile represents a spacing residue that keeps both Leu and Phe in an orientation for optimal complementarity with the major lipophilic binding site.[16] Deletion of this residue results in 20-fold lower activity for CDK2A (RRLF, 20), thereby further demonstrating its importance. Not surprisingly, a similar affect was observed with CDK4A due to the similarity of the two major hydrophobic pockets. Extension of this sequence with glycine to generate the p107 pentapeptide sequence (RRLFG, 19) resulted in a slight potency gain, since the carboxylate group of this residue is in closer proximity to Arg250. It was hypothesized that replacement of the native Leu residue with its one carbon homolog, β-homoleucine, would provide additional flexibility for the Phe side chain to adopt greater complementarity with the major lipophilic site and therefore mimic the critical side chain and the Ile spacer residue in a single residue.[25] Inclusion of a β-amino acid should also provide better pharmacokinetic properties through decreased proteolytic degradation. The potency increase observed in the octapeptide p107 series in the Phe (4, Table 1) and especially the 3TA (5) contexts confirmed this. For the 3TA replacement, the dramatic improvement in binding observed suggests excellent complementarity of the thiophene side chain with the hydrophobic pocket. Furthermore, significant activity enhancements of greater than 10-fold occurred for the truncated peptide counterparts 21 and 22 (CDK2A binding relative to 9 and 19, Table 3), therefore warranting further investigation in the context of optimized inhibitors.

A peptide analog containing β-Leu and also N-methylphenylalanine (24) therefore resulted in greater potency relative to its counterpart 20 in both the C-terminal acid and amide context (25). N-methylation of amino acids and their incorporation into peptides have been shown to promote cell permeability by removing the amide H-bond donor, thus

decreasing the desolvation penalty occurring during transduction through a biological membrane while imparting improved lipid solubility by addition of the hydrophobic methyl group. N-methylation also imparts greater resistance to degradation, since tertiary amides are poor substrates for protease enzymes.[27]

Through the verification that incorporation of the non-natural amino acids designed to improve stability and druglikeness, into the C-terminal motif, resulted in enhanced activity of binding to the cyclin groove, these substitutions were combined with the N-capping groups previously identified.[18] 27 and 28 included the 35DCPT group and NMePhe and 3TA, respectively, as the phenylalanine replacement (Figure 3 and Table 3). Of these two compounds, inclusion of the thiophene side chain (28) was found to generate a 2-fold advantage in activity compared to the N-methylPhe (27). This results from greater complementarity of the sulfur containing ring with the primary hydrophobic pocket relative to the phenyl side chain. Since both of these compounds have substantially reduced tPSA (220, 28, vs 303, 9) increased ClogP (2.57, 28, vs −2.75, 9) and considerably fewer H-bond acceptors and donors (Table 3), their druglike properties are dramatically enhanced relative to the native p21 pentapeptide (according to Lipinski's and other guidelines for oral drugs, tPSA should be less than 140 Å and ClogP between −0.4 and 5.6) The effectiveness of these compounds in cellular antiproliferative assays and therefore their ability to cross the biological membrane and induce cell death confirmed the validity of design and incorporation of druglike functionality (Table 3). Although the modified arginine residues substituted into the 28 scaffold generated compounds of similar or even better binding potency, improved cellular activity was unexpectedly not observed. The requirement for the free guanidine group suggests that steric hindrance may preclude interaction with the negatively charged headgroups of the bilayer and prevent the initial interactions required for transduction across the membrane. Although 29−32 series did not enhance cellular activity relative to 28, it is reassuring that the two most active inhibitors showed the best antiproliferative activity of the four tested. The observation that the lead compound 28 resulted in a significant G1 blockage (Figure 4), a cell cycle effect consistent with CDK2 and CDK4 inhibition through the cyclin groove, demonstrates on-target effects of this novel approach to cancer therapeutic development. Furthermore, these data confirm that REPLACE is an effective strategy for the iterative conversion of potent peptide inhibitors into compounds that are more appropriate for drug development.

■ MATERIALS AND METHODS

Peptide and FLIP Synthesis. All N-terminally capped FLIPs were synthesized and purified using standard Fmoc chemistry by GenScript (Piscataway, NJ). HPLC and MS were used to confirm the purity and structure of each peptide (Supporting Information Table 2). Peptides were assembled by using standard solid-phase synthesis methods. A sample procedure is given as follows: an amount of 5 equiv of the C-terminal amino acid (e.g., Fmoc-Phe, 202.7 mg, 0.5 mmol) was coupled to Rink resin (200 mg, 0.1 mmol) after activation with diisopropylethylamine (DIPEA) (6 equiv, 77.54 mg, 0.6 mmol) and HBTU (4.4 equiv, 166.86 mg, 0.58 mmol) in 2 mL of DMF for 1 h. The Fmoc protecting group of the C-terminal amino acid was removed using 20% piperidine in 3 mL of DMF for 10 min before addition of 5 equiv of the next amino acid using DIEA (0.082 mL) and HBTU (189.6 mg) in 5 mL of DMF. Wash cycles (5 × 10 mL of DMF + 5 × 10 mL of DCM) were applied to each step between coupling

and deprotection of Fmoc. Upon completion of assembly, side chain protecting groups were removed, and peptides were cleaved from Rink resin using (2 mL) 90:5:5 mixtures of TFA/H$_2$O/TIPS. Crude peptides were purified using reverse-phase flash chromatography and semipreparative reverse-phase HPLC methods. Pure compounds were lyophilized and characterized using mass spectrometry and analytical HPLC (see Supporting Information Table 1).

Energy Minimization and Interaction Energy Calculation. Modeled complexes of peptidic cyclin groove inhibitors bound to cyclin A were generated using the following protocol which has previously been validated:[18,22] The crystal structure of RRLIF (PDB code 1OKV) bound to cyclin A was used as the starting point following which Arg4 was mutated to the corresponding residue to generate cyclin groove bound complexes for compounds 9, 10, 11, 13, and 16 (Table 2). All calculations were performed using Discovery Studio 3.0 and specifically using the Macromolecules and Simulations protocols. Prior to minimization, the heavy atoms of the protein were set as constraints, and the CHARMm force field was applied to the receptor−ligand complex. For the energy minimization of the inhibitor cyclin complex, the Smart Minimizer algorithm was used with 2000 minimization iterations and a convergence criterion of 0.1 (rms gradient). The routine also employed the GBSW[28] (generalized Born with a simple switching) implicit solvent model using a dielectric constant of 1 and an implicit solvent dielectric constant of 80 with all other parameters being set as default. After minimization of the complex to convergence, the interaction energy between cyclin A and each peptide was calculated using the receptor−ligand interaction module again using the GBSW implicit solvent model. Calculated interaction energy values are shown in Supporting Information Table 1.

Cell Culture. U2OS osteosarcoma cells and DU145 human prostate cancer cell lines were obtained from ATCC (Manassas, VA). All cells were grown in Dulbecco's modified Eagle medium (DMEM, Fisher Scientific) supplemented with 10% fetal bovine serum (FBS, USA Scientific) and 100 μg/mL streptomycin (strep)/100 U/mL penicillin (pen). Cells were incubated at 37 °C with 5% CO$_2$.

Viability Assay. Cells were seeded in 96-well plates at (2×10^3 cells/mL) and allowed to adhere overnight in DMEM growth medium containing 10% NU serum and 1% pen/strep. The compounds 26, 27, and 28 were dissolved in DMSO and added in a dose dependent manner (1−100 μM). The diluted compounds were added to the cells in triplicate and incubated for 72 h at 37 °C with 5% CO$_2$. The cell viability was determined using MTT (3-(4,5-dimethylthiazol-2-yl)-2,5-diphenyltetrazolium bromide) assay.[29] Absorbance readings were obtained using a DTX880 multimode detector fitted with 595 nm filter. Cell viability results were represented as the ratio of the absorbance reading in treated vs untreated cells. IC$_{50}$ values were obtained using a nonlinear regression line with GraphPad Prism 5.0. Experiments were performed in triplicate.

Cell Cycle Analysis. Cells were plated at 150 000 cells/mL overnight in six-well plates. CDK2 inhibitors were added in a dose dependent fashion for 48 h. The cells were then fixed with 70% ethanol overnight at −20 °C. The cells were centrifuged, and ethanol was removed. The cells were washed twice with 1× PBS following staining with DAPI (4′,6′ diamino-2-phenylindole) and analyzed using BD LSR II (Becton Dickenson) with a blue filter. Experiments were performed in triplicate.

Fluorescence Polarization Binding Assay. *CDK4D1 FP Assay.* This assay was performed using black 384-well plates using a previously described procedure[30] with the following modifications. To each well were added the following: 5 μL of CDK4D1 (0.5 μg/well purified recombinant human kinase complex from BPS Bioscience), 5 μL of compound solution, 5 μL of 12 nM fluoresceinyl-Ahx-Pro-Val-Lys-Arg-Arg-Leu-(3ClPhe)-Gly tracer peptide. Compounds and kinase complexes were diluted using assay buffer (25 nM HEPES, pH 7, 10 nM NaCl, 0.01% Nonidet P-40, 1 mg/ml BSA, 1 mM dithiothretiol (DTT)). Plate was centrifuged for 1 min at 500 rpm and then incubated with shaking for 45 min at room temperature. Fluorescence polarization was read on DTX880 multimode detector (Beckman Coulter, Brea, CA) fitted with 485 nm/535 nm excitation/emission

filters and a dichroic mirror suitable for fluorescein. Relative mp was calculated for each concentration tested using the equation showing below. IC$_{50}$ values were determined by logarithmic regression by correlating relative melting points and testing concentrations.

$$\text{relative mp} = \frac{\text{mp(compound)} - \text{mp(DMSO, protein, tracer)}}{\text{mp(DMSO, protein)} - \text{mp(DMSO, protein, tracer)}}$$

CDK2A2 FP Assay. This assay was performed using black 384-well plates. To each well were added the following: 5 μL of CDK2A2 (0.27 μg/well purified recombinant human kinase complex), 5 μL of compound solution, 5 μL of 12 nM fluoresceinyl-Ahx-Pro-Val-Lys-Arg-Arg-Leu-(3ClPhe)-Gly tracer peptide. Compounds and kinase complexes were diluted using assay buffer (25 nM HEPES, pH 7, 10 nM NaCl, 0.01% Nonidet P-40, 1 mg/ml BSA, 1 mM dithiothretiol (DTT)). Plate was centrifuged for 1 min at 500 rpm and then incubated with shaking for 45 min at room temperature. Fluorescence polarization was read on DTX880 multimode detector (Beckman Coulter, Brea, CA) fitted with 485 nm/535 nm excitation/emission filters and a dichroic mirror suitable for fluorescein. Relative mp was calculated for each concentration tested using the equation showing above. IC$_{50}$ values were determined by logarithmic regression by correlating relative melting points and testing concentrations.

Determination of Dissociation Constant (K_d) from Fluorescence Measurements of Cyclin A2 Binding Activity. For the binding assay of 6xHis-cyclin A2 with compound 8, a previously developed method was exploited[31] in order to determine the dissociation constant (K_d) of recombinant cyclin A2 with the ligand. Differences in fluorescence intensity at 345 nm between the complex (cyclin A2/compound 8) and free protein (excitation at 295 nm) were analyzed by measuring the respective fluorescence intensities with a Hitachi F-2500 fluorescence spectrophotometer in 0.4 cm × 1 cm quartz cuvettes at 25 °C. The excitation and emission wavelengths were 295 and 345 nm, respectively. The slits were set at 5 and 20 nm for the excitation and emission, respectively. Briefly, 1.5 mL of protein solution in fluorescence buffer (0.1–0.65 μM) was equilibrated in a cuvette at 25 °C for 1 h. After equilibration, small increments (2–10 μL) of the ligand solution were injected and binding was allowed to take place for 2 min, with shutter closed to avoid protein deterioration, before fluorescence intensity measurement. In order to determine the mandatory dilution effect due to the addition of ligand and any fluorescence effect due to the unbound ligand, a blank sample containing tryptophan with fluorescence signal of a similar level was titrated with the addition of the exact ligand injections. Measured intensities were corrected for blank signals. The corresponding K_d values of the binding reactions were determined using Prism (GraphPadSoftware, San Diego, CA).

ASSOCIATED CONTENT

Ⓢ Supporting Information

One table providing analytical characterization data for FLIPs shown in Tables 1–3; one table showing the calculated data for the interaction energies plotted in Figure 2; one figure showing the plot and calculated data for the measurement of direct binding affinity of HAKRRLIF to cyclin A using intrinsic tryptophan fluorescence. This material is available free of charge via the Internet at http://pubs.acs.org.

AUTHOR INFORMATION

Corresponding Author
*E-mail: mcinnes@sccp.sc.edu. Phone: (803) 576-5684.

Present Address
§S.L.: Department of Surgery, University of California at San Francisco, San Francisco, CA. E-mail, shu.liu@ucsfmedctr.org.

Notes
The authors declare the following competing financial interest(s): C.M. recently formed a company that aims to commercialize future versions of the compounds described herein.

REFERENCES
(1) Shapiro, G. I. Cyclin-dependent kinase pathways as targets for cancer treatment. *J. Clin. Oncol.* **2006**, *24*, 1770–1783.
(2) Sherr, C. J. Cancer cell cycles. *Science* **1996**, *274*, 1672–1677.
(3) Malumbres, M.; Barbacid, M. To cycle or not to cycle: a critical decision in cancer. *Nat. Rev. Cancer* **2001**, *1*, 222–231.
(4) Ball, K. L.; Lain, S.; Fåhraeus, R.; Smythe, C.; Lane, D. P. Cell-cycle arrest and inhibition of Cdk4 activity by small peptides based on the carboxy-terminal domain of p21^{WAF1}. *Curr. Biol.* **1997**, *7*, 71–80.
(5) Chen, J. S. P.; Kornbluth, S.; Dynlacht, B. D.; Dutta, A. Cyclin-binding motifs are essential for the function of p21CIP1. *Mol. Cell. Biol.* **1996**, *16*, 4673–4682.
(6) Kitagawa, M.; Higashi, H.; Suzuki-Takahashi, I.; Segawa, K.; Hanks, S. K.; Taya, Y.; Nishimura, S.; Okuyama, A. Phosphorylation of E2F-1 by cyclin A-cdk2. *Oncogene* **1995**, *10*, 229–236.
(7) Phillips, A. C.; Vousden, K. H. E2F-1 induced apoptosis. *Apoptosis* **2001**, *6*, 173–182.
(8) Chen, Y. N.; Sharma, S. K.; Ramsey, T. M.; Jiang, L.; Martin, M. S.; Baker, K.; Adams, P. D.; Bair, K. W.; Kaelin, W. G., Jr. Selective killing of transformed cells by cyclin/cyclin-dependent kinase 2 antagonists. *Proc. Natl. Acad. Sci. U.S.A.* **1999**, *96*, 4325–4329.
(9) Mendoza, N.; Fong, S.; Marsters, J.; Koeppen, H.; Schwall, R.; Wickramasinghe, D. Selective cyclin-dependent kinase 2/cyclin A antagonists that differ from ATP site inhibitors block tumor growth. *Cancer Res.* **2003**, *63*, 1020–1024.
(10) Mendoza, N.; Severin, C.; Marsters, J.; Wickramasinghe, D. Cyclin A antagonists kill tumor cells in vitro and in vivo. *Proc. Am. Assoc. Cancer Res.* **2004**, *45*, 834.
(11) Tetsu, O.; McCormick, F. Proliferation of cancer cells despite CDK2 inhibition. *Cancer Cell* **2003**, *3*, 233–245.
(12) Malumbres, M.; Barbacid, M. Is Cyclin D1-CDK4 kinase a bona fide cancer target? *Cancer Cell* **2006**, *9*, 2–4.
(13) Malumbres, M.; Sotillo, R.; Santamaria, D.; Galan, J.; Cerezo, A.; Ortega, S.; Dubus, P.; Barbacid, M. Mammalian cells cycle without the D-type cyclin-dependent kinases Cdk4 and Cdk6. *Cell* **2004**, *118*, 493–504.
(14) Lam, L. T.; Pickeral, O. K.; Peng, A. C.; Rosenwald, A.; Hurt, E. M.; Giltnane, J. M.; Averett, L. M.; Zhao, H.; Davis, R. E.; Sathyamoorthy, M.; Wahl, L. M.; Harris, E. D.; Mikovits, J. A.; Monks, A. P.; Hollingshead, M. G.; Sausville, E. A.; Staudt, L. M. Genomic-scale measurement of mRNA turnover and the mechanisms of action of the anti-cancer drug flavopiridol. *Genome Biol.* **2001**, *2*, research0041.1–0041.11.
(15) Lu, X.; Burgan, W. E.; Cerra, M. A.; Chuang, E. Y.; Tsai, M. H.; Tofilon, P. J.; Camphausen, K. Transcriptional signature of flavopiridol-induced tumor cell death. *Mol. Cancer Ther* **2004**, *3*, 861–872.
(16) Zheleva, D. I.; McInnes, C.; Gavine, A.-L.; Zhelev, N. Z.; Fischer, P. M.; Lane, D. P. Highly potent p21^{WAF1} derived peptide inhibitors of CDK-mediated pRb phosphorylation: delineation and

structural insight into their interactions with cyclin A. *J. Pept. Res.* **2002**, *60*, 257−270.

(17) McInnes, C.; Andrews, M. J.; Zheleva, D. I.; Lane, D. P.; Fischer, P. M. Peptidomimetic design of CDK inhibitors targeting the recruitment site of the cyclin subunit. *Curr. Med. Chem.: Anti-Cancer Agents* **2003**, *3*, 57−69.

(18) Liu, S.; Premnath, P. N.; Bolger, J. K.; Perkins, T. L.; Kirkland, L. O.; Kontopidis, G.; McInnes, C. Optimization of non-ATP competitive CDK/cyclin groove inhibitors through REPLACE-mediated fragment assembly. *J. Med. Chem.* **2013**, *56*, 1573−1582.

(19) McInnes, C. Progress in the development of non-ATP competitive protein kinase inhibitors for oncology. In *Annual Reports in Medicinal Chemistry*; Bernstein, P, Desai, M., Ed.; Elsevier: Amsterdam, 2012; Vol. 47, pp 459−474.

(20) Andrews, M. J.; Kontopidis, G.; McInnes, C.; Plater, A.; Innes, L.; Cowan, A.; Jewsbury, P.; Fischer, P. M. REPLACE: a strategy for iterative design of cyclin-binding groove inhibitors. *ChemBioChem* **2006**, *7*, 1909−1915.

(21) Premnath, P. N.; Liu, S.; Perkins, T.; Abbott, J.; Anderson, E.; McInnes, C. Fragment based discovery of arginine isosteres through REPLACE: towards non-ATP competitive CDK inhibitors. *Bioorg. Med. Chem.* **2014**, *22*, 616−622.

(22) Liu, S.; Bolger, J. K.; Kirkland, L. O.; Premnath, P. N.; McInnes, C. Structural and functional analysis of cyclin D1 reveals p27 and substrate inhibitor binding requirements. *ACS Chem. Biol.* **2010**, *5*, 1169−1182.

(23) Kontopidis, G.; Andrews, M. J. I.; McInnes, C.; Cowan, A.; Powers, H.; Innes, L.; Plater, A.; Griffiths, G.; Paterson, D.; Zheleva, D. I.; Lane, D. P.; Green, S.; Walkinshaw, M. D.; Fischer, P. M. Insights into cyclin groove recognition: complex crystal structures and inhibitor design through ligand exchange. *Structure* **2003**, *11*, 1537−1546.

(24) Castanedo, G.; Clark, K.; Wang, S.; Tsui, V.; Wong, M.; Nicholas, J.; Wickramasinghe, D.; Marsters, J. C., Jr.; Sutherlin, D. CDK2/cyclinA inhibitors: targeting the cyclinA recruitment site with small molecules derived from peptide leads. *Bioorg. Med. Chem. Lett.* **2006**, *16*, 1716−1720.

(25) Kontopidis, G.; Andrews, M. J.; McInnes, C.; Plater, A.; Innes, L.; Renachowski, S.; Cowan, A.; Fischer, P. M. Truncation and optimisation of peptide inhibitors of cyclin-dependent kinase 2-cyclin a through structure-guided design. *ChemMedChem* **2009**, *4*, 1120−1128.

(26) Kennedy, K. J.; Lundquist, J. T. I.; Simandan, T. L.; Kokko, K. P.; Beeson, C. C.; Dix, T. A. Design rationale, synthesis, and characterization of non-natural analogs of the cationic amino acids arginine and lysine. *J. Pept. Res.* **2000**, *55*, 348−358.

(27) Chatterjee, J.; R, F.; Kessler, H. N-methylation of peptides and proteins: an important element for modulating biological functions. *Angew. Chem., Int. Ed.* **2013**, *52*, 254−269.

(28) Khandogin, J.; Brooks, C. L., 3rd. Constant pH molecular dynamics with proton tautomerism. *Biophys. J.* **2005**, *89*, 141−157.

(29) Denizot, F.; Lang, R. Rapid colorimetric assay for cell growth and survival. Modifications to the tetrazolium dye procedure giving improved sensitivity and reliability. *J. Immunol. Methods* **1986**, *89*, 271−277.

(30) Andrews, M. J.; McInnes, C.; Kontopidis, G.; Innes, L.; Cowan, A.; Plater, A.; Fischer, P. M. Design, synthesis, biological activity and structural analysis of cyclic peptide inhibitors targeting the substrate recruitment site of cyclin-dependent kinase complexes. *Org. Biomol. Chem.* **2004**, *2*, 2735−2741.

(31) Papaneophytou, C. P.; Grigoroudis, A. I.; McInnes, C.; Kontopidis, G. Quantification of the effects of ionic strength, viscosity, and hydrophobicity on protein-ligand binding affinity. *ACS Med. Chem. Lett.* **2014**, *5*, 931−936.